Long-range transport and universality classes in *in vitro* viral infection spread

S. C. MANRUBIA[1], J. GARCÍA-ARRIAZA[2], E. DOMINGO[1,2] and C. ESCARMÍS[2]

[1] *Centro de Astrobiología, CSIC-INTA - Ctra. de Ajalvir km. 4*
28850 Torrejón de Ardoz, Madrid, Spain
[2] *Centro de Biología Molecular Severo Ochoa, CSIC-UAM - Universidad Autónoma de Madrid - Cantoblanco, 28049 Madrid, Spain*

Abstract. – Dispersal mechanisms play a main role in the dynamics of infection spread. Recent experimental results with *in vitro* infections of foot-and-mouth disease virus reveal that the time needed for the virus to kill a cellular monolayer depends qualitatively on the number of viral particles required to initiate infection in a susceptible cell. A two-dimensional susceptible-infected-removed (SIR) model based on the experimental setting agrees with the observations only when viral particles are subject to long-range transport. Numerical and analytical results show that this long-range transport plays a role when a single particle causes infection, while it is inefficient when complementation between two or more particles is necessary.

The knowledge of the mechanisms involved in disease spread determines our ability to control the dynamics of epidemics in natural populations [1,2]. Decades of study in this field show that the fate of an exposed population depends on many factors, among others the way in which the pathogen is transmitted [3], the connectivity patterns among individuals [4], or the dimensionality of the physical space where propagation occurs [5]. The specific environment where infection originates and spreads, together with the transmission mechanism and the characteristics of the host, define different scenarios where epidemics outbreaks occur with broadly variable probability [6].

Since real populations rarely behave as a well-mixed system or as a purely diffusive one, the role played by long-range dispersal mechanisms (added to local diffusion) in the development of epidemics has been an issue of study [3,7–10]. It is known that long-range dispersal changes the properties of the process qualitatively [11,12]. In this letter, we present experimental, numerical, and analytical results concerning the spread of a viral infection on a cellular monolayer. The *in vitro* system shares many features with models of disease spread. The use of two qualitatively different viral forms demonstrates indirectly that, as expected, short- and long-range transport belong to different universality classes.

Complementation refers to the interaction between virus gene products or gene products and genomes of two different parental viruses coinfecting the same cell: one of the viruses provides a functional gene product for another virus that lacks that function. This mechanism
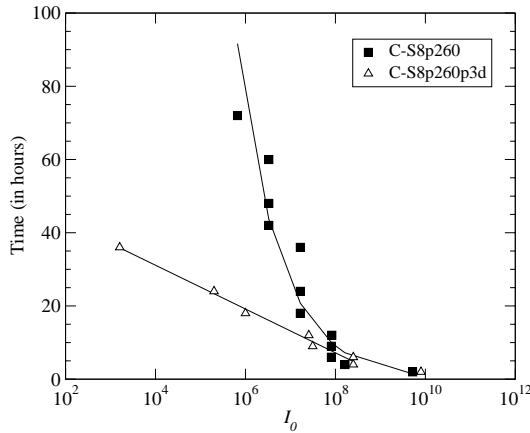
Fig. 1 – Dependence of the time T required to kill a cellular monolayer of baby hamster kidney cells on the initial number of viral particles I_0. After 260 passages at high MOI, the segmented form C-S8p260 is selected (see main text). This transition can be reverted with passages at low MOI, such that the form C-S8p260p3d with a complete genome is the major form after only three additional passages of C-S8p260 at low MOI [16]. The continuous curves are least-squares fit to the data. Regression coefficients are $\beta = -0.46(5)$, $b = 10.7(8)$, and $r = -0.96$ for C-S8p260; $\alpha = -2.3(2)$, $a = 52(3)$, and $r = -0.98$ for C-S8p260p3d.

influences evolutionary features of viral populations [13–15]. It was recently observed that under serial passages carried out at high multiplicity of infection (MOI: number of infectious particles per cell), a wild-type variant of the foot-and-mouth disease virus (FMDV) spontaneously generated two forms with incomplete genomes, each encapsidated in a different viral particle [16]. These two types of virions are defective and infection can only occur by complementation between them, that is only when at least one particle of each type enters a cell.

The relative performance of wild-type (w, unsegmented form) *vs.* defective (s, segmented form) virus can be quantified through cell killing assays, an experimental protocol used to quantify virulence. A monolayer of susceptible cells which occupy fixed positions on a surface is infected with a controlled number of viral particles. The virus replicates its genetic material inside each infected cell and, once the infection cycle is completed, the cell is lysed (killed). Thousands of new viral particles are then released to a liquid medium that covers the cellular monolayer and allows them to diffuse freely. For the virus used, about one in 10^4 particles produced is infectious. From another viewpoint, this translates into a typical time to infect a cell notably larger than that required to diffuse on the plate. As a consequence, while cells adjacent to recently lysed ones are infected almost with certainty, distant cells can be infected with a (low) near constant probability(^{1}). The cycle repeats when new susceptible cells are infected. The killing process ends at time T, when the N cells in the monolayer have been lysed by the virus. The relation between T and the initial amount of infecting viral particles c_0 quantifies the ability of the virus to produce and spread infections in that environment. The total number of viral particles initially added to the system, which can be experimentally measured, is $I_0 \simeq 10^4 c_0$ (see fig. 1).

(^{1})The time required for a viral particle to adsorb to the cell and penetrate through the membrane is about 30 to 60 minutes, and the time to complete an infectious cycle inside the cell and release the progeny ranges from 2 to 4 hours. Through pure diffusion, a viral particle (of 30 nm diameter) requires 1 second to cover the distance equivalent to one cell (10 μm; the experiments where performed at a temperature of 310 K). The presence of chemical gradients and the spreading of particles caused when the cell lyses add to homogeneize the liquid layer.

In the assays carried out with FMDV, a logarithmic dependence of the form $T \propto \alpha \ln I_0 + a$ is observed for wild-type particles, while the case of segmented genomes that require complementation yields $\ln T \propto \beta \ln I_0 + b$ (fig. 1). Since the experimental setting is exactly the same for both forms of the virus, the qualitatively different behaviors can only be ascribed to the requirement of complementation between particles to cause infection.

From the viewpoint of epidemics, the infection process can be modeled as a SIR model with an absorbing state when all of the individuals are in the R state. At time $t = 0$, $n(0)$ cells become infected. If we assume that there is an equal number of particles belonging to each of m classes, and that infection occurs only when at least one particle of each class infects a cell, $n(0)$ is given by

$$n(0) = N \left(1 - \exp[-c_0/(mN)]\right)^m , \tag{1}$$

where N is the total number of cells to be killed. The number of viral particles of each type infecting a cell follows a Poisson distribution of average $c_0/(mN)$, such that $m = 1$ and 2 stand for w and s particles, respectively. From now on, we use $n(0)$ to describe the process[2]. In the experimental assays, either all particles were wild-type or the two segmented, complementary forms were simultaneously present, without w particles.

The infection cycle in a cell ends when enough viral particles have been produced such that the cell is lysed and $k \simeq 1$ viral particles effectively infect new cells. If a particle belonging to the wild type enters a susceptible cell, the cell becomes immediately infected. However, if the particle contains a defective genome and requires complementation, infection occurs only when a second particle of the complementary type enters the same cell. The infection proceeds until a time $t = T$, at which all cells in the monolayer are killed

$$n(T) = N , \tag{2}$$

where $n(t)$ is the number of cells killed at time t. We are interested in the relation between T and $n(0)$, the latter indirectly derived from direct measures of I_0.

In the framework of the SIR model, the transition $S \to I$ occurs with rates $p_w(t)$ and $p_s(t)$ that depend on the viral form infecting the cell (w or s), on the properties of the environment, and on time, while the transition $I \to R$ occurs with probability one when the infection cycle ends and the cell is lysed by the virus.

Mean-field analysis. –   Infection spread by wild-type and defective particles can be first studied in a simple situation of perfect mixing of particles. In this case,

$$\begin{aligned}
p_w(t) &= k_w \frac{n(t) - n(t-1)}{N - n(t)}, \\
p_s(t) &= \left(\frac{k_s}{2}\right)^2 \left(\frac{n(t) - n(t-1)}{N - n(t)}\right)^2 ,
\end{aligned} \tag{3}$$

where $N - n(t)$ is the amount of cells in the S state at time t, and the number of viral particles produced is $k_{w,s}$ times the number of cells lysed at time t, and where the subindexes stand for w and s particles. Note that the difference $n(t) - n(t-1)$ corresponds to the derivative at time $t - 1$, so eqs. (3) can be viewed as conservation equations. The threshold for spreading of the infection results from the condition that at least one cell is killed at each time step. For w particles the condition is trivial and simply implies that the basic reproductive number

---

[2] $n(0)$ is called *number of plaque forming units* or PFU by the virological community. It is estimated by counting of lytic plaques in the experiments; $I_0 \simeq 10^4 c_0$ is quantified through real-time polymerase chain reaction.

k_w has to be larger than one (one assumes $n(0) \geq 1$). For s particles the condition $n(t) \geq 1$ for all t is particularly demanding at the initial time steps due to the high dilution of the particles. If $n(1) > 1$, for $n(0)$ given, the infection will spread, since $n(t)$ is non-decreasing. This imposes a strong limit on the production of viruses,

$$k_s \geq 2\sqrt{N-1}, \tag{4}$$

and sets a limit on the initial number of viral particles as well, $c_0 \geq k_s$ for $n(0)$ to be larger than one. The conditions on c_0 and $k_{w,s}$ represent the threshold conditions for invasion and endemicity of the infection, respectively.

In this scenario, the kinetics of the infection follows:

$$n(t+1) = n(t) + p_{w,s}(N - n(t)) \tag{5}$$

with $p_{w,s}$ given in eq. (3) and the initial condition $n(0)$ and $n(1) = (1 + k_w n(0))$. Equation (5) is easily solvable for w particles, and condition (2) yields a dependence of the form $T_w \propto -\ln n(0)$. For s particles, the kinetics can be solved in a time-continuous approximation, described by the differential equation

$$\frac{\mathrm{d}n(t)}{\mathrm{d}t} + \frac{1}{2}\frac{\mathrm{d}^2 n(t)}{\mathrm{d}t^2} = \frac{k_s^2}{4(N - n(t))}\left(\frac{\mathrm{d}n(t)}{\mathrm{d}t}\right)^2. \tag{6}$$

This equation has a solution of the form $t = c_2 - \ln[2(n(t) - N)^{1+k_s^2/2} - c_1(1 + k_s^2/2)]/2$, where c_1 and c_2 are determined from $n(0)$ and $n'(0) = n(0)/\sqrt{2}$. Applying eq. (2), the relation between the time of complete cell killing and the initial number of viral particles takes again the functional form $T_s \propto -\ln n(0)$.

Hence, this mean-field approximation yields the same functional form for the dependence between T and $n(0)$ in the wild-type and in the segmented genome cases, and thus does not capture the qualitative difference observed empirically. Moreover, it sets a strong limit on the spreading of infection for s particles, since k_s turns out to depend on the system size N.

Two-dimensional model. – Let us now consider the SIR process on a two-dimensional lattice. Each cell is placed on a site of the lattice, and the particles released upon lysis diffuse to the eight nearest neighbors. We consider a long-range transport mechanism as well. This mimics the fact that the cellular monolayer is covered by a liquid medium that transports a small fraction of particles far from their origination site. In our model, a viral particle can infect a randomly chosen susceptible cell anywhere in the two-dimensional lattice with a probability $q \ll 1$. Some features of this kind of dispersal have been studied in previous works [7], and the deep analogy between long-range transport and small-world properties in systems of mobile individuals has been put forward [9,11].

We consider first the growth of a single infectious focus ($n(0) = 1$), with $q = 0$. After a few cycles where the number of removed cells increases exponentially, the radial growth of the lytic plaque saturates and the number of newly infected cells becomes proportional to the perimeter of the plaque. Using a space-continuous approximation, we expect a kinetics of the form $n(t+1) \simeq n(t) + 2\pi\sqrt{n(t)/\pi}$. In this regime, the number of lysed cells grows asymptotically as the square of time, $n(t) \simeq \pi t^2$, and does not depend qualitatively on the type of particles. If many independent cells initiate the infection, then $N/n(0)$ cells have to be killed per lytic plaque, such that T is given by

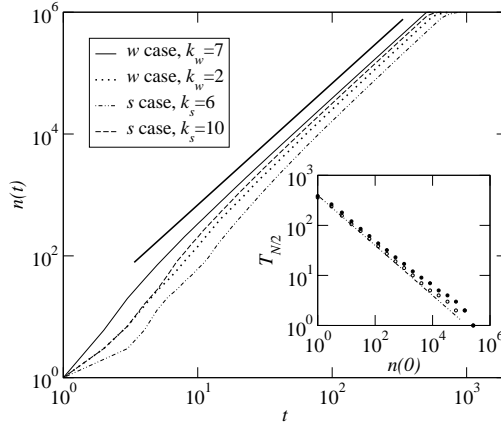$$2\ln T \simeq -\ln n(0) + \ln(N/\pi). \tag{7}$$

Fig. 2 – Main plot: kinetics of growth of a single lytic plaque in the two-dimensional model with diffusion to nearest neighbors. After a few infection cycles, the number $n(t)$ of lysed cells grows proportionally to t^2 (the bold solid line has slope 2), irrespectively of the form of the virus. The basic reproductive number corresponding to each curve and case is shown in the legend. Insert: time $T_{N/2}$ required to kill $N/2 = 5 \times 10^5$ cells in a square lattice for cases w and s (open and solid circles, respectively, $k_w = 5$, $k_s = 10$). The dot-dashed curve is $2 \ln T \simeq -\ln n(0) + \ln(N/(2\pi))$, which works better for larger plaques (small $n(0)$), since their shape is closer to circular.

We represent in fig. 2 the simulation time $T_{N/2}$ required to kill $N/2$ cells (this is to minimize finite-size effects due to plaque merging) together with the corresponding prediction. w and s particles behave similarly, so single-plaque growth, dominated by short-range dispersal, cannot account for the qualitative differences observed in the experiments.

The situation changes when $q \neq 0$. Long-range jumps represent directed, random links shortcutting the transmission of the disease between an arbitrary pair of sites. Suppose that, initially, a single cell is killed, and originates a lytic plaque which grows as $n(t) \simeq \pi t^2$. This proceeds until a characteristic time $t_1 = (k\pi q)^{-1/2}$ when, on average, one of the newly generated viral particles infects a randomly chosen cell anywhere in the monolayer. This second plaque grows as $n'(t) \simeq \pi(t - t_1)^2$. In general, the total number of cells lysed through this procedure is

$$n(t) \simeq \pi \sum_{i=0}^{k-1} (t_k - t_i)^2 \,, \tag{8}$$

and the discrete times t_k at which the k-th plaque starts to grow are implicitly defined through the equation

$$t_1^2 = \sum_{i=0}^{k-1} \left[(t_k - t_i)^2 - (t_{k-1} - t_i)^2 \right] \,. \tag{9}$$

If we consider the new variable $\tau_k = (t_k - t_{k-1})/t_1$, a solution of the form $k\tau_k = c + \epsilon_{k-1} + \epsilon_k$, with $c = 1/\sqrt{2}$ and $\epsilon_0 = c/2$ satisfies eq. (9). In the original variables t_k, this yields

$$t_k \simeq t_1 \left(\frac{1}{\sqrt{2}} (\gamma + \ln k) + B - \frac{C}{k^2} \right) \,, \tag{10}$$

where $\gamma = 0.5772\ldots$ is Euler's constant, $B = 0.3124\ldots$, and $C = 0.0337\ldots$. We first calculate
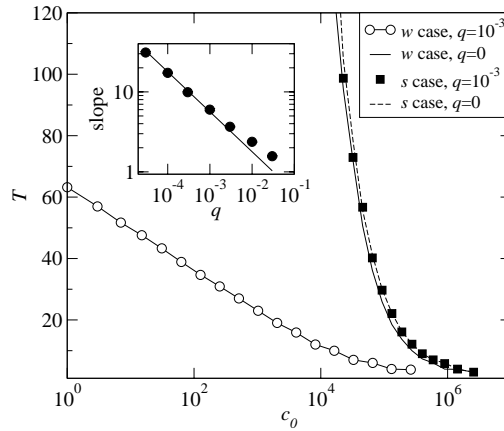
Fig. 3 – Time to complete cell killing for w and s particles when $q \neq 0$. The qualitative dependence of T on c_0 changes in the wild-type case, where long-range dispersal is efficient. This contrasts with the segmented case, where only local diffusion is relevant to spread the infection. For $c_0 \to \infty$ the curves saturate at $T = 1$. Compare these results with the experimental observations depicted in fig. 1. Insert: comparison between the numerical slopes in the w case for several values of q (solid circles) and the theoretical prediction of eq. (13) (solid line).

the derivative of $n(t)$, corresponding to the number of cells killed at timestep t. From eq. (8),

$$\frac{1}{2\pi}\frac{dn(t)}{dt} = \sum_{i=0}^{k-1}(t_k - t_i) = t_1 \sum_{i=1}^{k} i\tau_i \,. \tag{11}$$

Inverting eq. (10), substituting in eq. (11), and integrating, we obtain the large time behavior of $n(t)$,

$$n(t) \simeq \pi t_1^2 \exp\left[\sqrt{2}\left(\frac{t}{t_1} - D\right)\right] + \mathrm{O}(t^{-1}) \,, \tag{12}$$

with $D = 0.7205\ldots$. As in the case $q = 0$, we can assume that the infectious process ends once each initial plaque and the new plaques it has generated through long-range jumps have killed an average of $N/n(0)$ cells. This condition finally yields the sought dependence of T on $n(0)$,

$$\sqrt{2k\pi p}\, T \simeq -\ln n(0) + \ln(kqN) \,. \tag{13}$$

Figure 3 compares numerical results for w and s particles and $q \neq 0$ with the theoretical predictions. The killing time T is represented as a function of the initial number of particles c_0, which is related to $n(0)$ through eq. (1). This allows a direct comparison with the experiments shown in fig. 1. In particular, for $c_0 \ll mN$, $c_0 \simeq n(0)$ for w particles, and $c_0 \simeq 2\sqrt{Nn(0)}$ for s particles, so the funcional dependence is not changed. The fit of experimental data yields coefficients $\sqrt{2k\pi q}$ between 2 and 3.5 for w particles. This implies that the product $kq \sim \mathrm{O}(10^{-2})$. Empirical evidence suggests that $k \simeq 10$, so the weight of long-range transport with respect to local diffusion is of order 10^{-3}. However, in the case of segmented genomes, this value of q implies that long-range coinfection occurs proportionally to q^2/N, which is of order 10^{-11} for a typical (small) plate with $N = 10^5$ cells. In practice, its effects can be ignored. Infection spread with a segmented virus is thus better described with $q = 0$, such that it is expected to follow eq. (7).

The mean-field description of the SIR process yields a fast spread of infection irrespectively of the particle type, and fails to capture the qualitative behavior of infection by s particles. The explicit representation of two-dimensional space slows down the process and changes the dependence between T and c_0. Long-range transport of particles is able to counterbalance this effect for w particles, where it is efficient, while infection by s particles is not affected by it. Thus, two-dimensional space plus long-range transport are the minimal ingredients required to explain the empirical observations.

Viruses with segmented genomes are mostly plant and fungi parasites. Once these organisms are infected, the disease proceeds throught the direct transmission of the pathogen from cell to cell, such that local diffusion is the main mechanism for infection spreading. Additionally, the transmission of viral infections in plant and fungi usually occurs under high MOI. These two mechanisms prevent a strong dilution of viral particles, thus conferring a selective advantage to s particles in those particular environments. In contrast, animal viruses undergo frequent population bottlenecks when jumping from host to host, thus experiencing states of high dilution that probably select against viral forms requiring complementation between particles [17]. The environment where pathogens evolve and the selection pressures they experience determine their functional characteristics. The examples discussed here highlight the importance of understanding viral properties and environmental features in order to better predict and eventually control epidemic diseases.

$$* * *$$

REFERENCES

[1] Diekmann O. and Heesterbeek J. A. P., *Mathematical Epidemiology of Infectious Diseases: Model Building, Analysis, and Interpretation* (Wiley & Sons, New York) 2000.
[2] Ferguson N. M., Keeling M. J., Edmunds W. J., Gani R., Greenfell B. T. and Anderson R. M., *Nature*, **425** (2003) 681.
[3] Filipe J. A. N. and Maule M. M., *J. Theor. Biol.*, **226** (2004) 125.
[4] Barthélemy M., Barrat A., Pastor-Satorras R. and Vespigniani A., *Phys. Rev. Lett.*, **92** (2004) 178701.
[5] Tuckwell H. C., Toubiana L. and Vibert J.-F., *Phys. Rev. E*, **64** (2001) 041918.
[6] Hethcote H. W., *SIAM Rev.*, **42** (2000) 599.
[7] Boccara N. and Cheong K., *J. Phys. A*, **25** (1992) 2447.
[8] Kuperman M. and Abramson G., *Phys. Rev. Lett.*, **86** (2001) 2909.
[9] Miramontes O. and Luque B., *Phys. D*, **168** (2002) 379.
[10] Newman M. E. J., Jensen I. and Ziff R. M., *Phys. Rev. E*, **65** (2002) 021904.
[11] Manrubia S. C., Delgado J. and Luque B., *Europhys. Lett.*, **53** (2001) 693.
[12] Janssen H. K., Oerding K., van Wijland F. and Hilhorst H. J., *Eur. Phys. J. B*, **7** (1999) 137.
[13] Turner P. E. and Chao L., *Nature*, **398** (1999) 441.
[14] Frank S. A., *Heredity*, **97** (2001) 522.
[15] Novella I. S., Reissig D. D. and Wilke C. O., *J. Virol.*, **78** (2004) 5799.
[16] García-Arriaza J., Manrubia S. C., Toja M., Domingo E. and Escarmís C., *J. Virol.*, **78** (2004) 11678.
[17] Chao L., *J. Theor. Biol.*, **153** (1991) 229.